

## Supporting Information:

# **An impedance method for spatial sensing of 3D cell constructs – towards applications in tissue engineering**

*Chiara Canali et al.*

### **Content:**

- S1:** Theory – Electrode configurations in bioimpedance measurements
- S2:** FE simulation of alternative measurement chamber size and electrode distance
- S3:** FE simulation of metal and plastic phantoms
- S4:** Summary of phantom experiments
- S5:** Biompedance sensing of 5% (w/v) bulk gelatin scaffolds
- S6:** Biompedance sensing of 5% (w/v) gelatin cylinders and artificial 3D cell constructs
  - S6A)** Gelatin cylinders without cells
  - S6B)** Artificial 3D cell constructs

## Section S1. Theory – Electrode configurations in bioimpedance measurements

The sensitivity field in bioimpedance measurements depends on several parameters, such as electrode number, geometry, orientation and spacing. Moreover, one crucial element to carefully consider is the used configuration between electrode couples (current carrying, CC, and voltage pick-up, PU). Two, three, four terminal (T) configurations may be used and they are illustrated in Fig. S1.1.

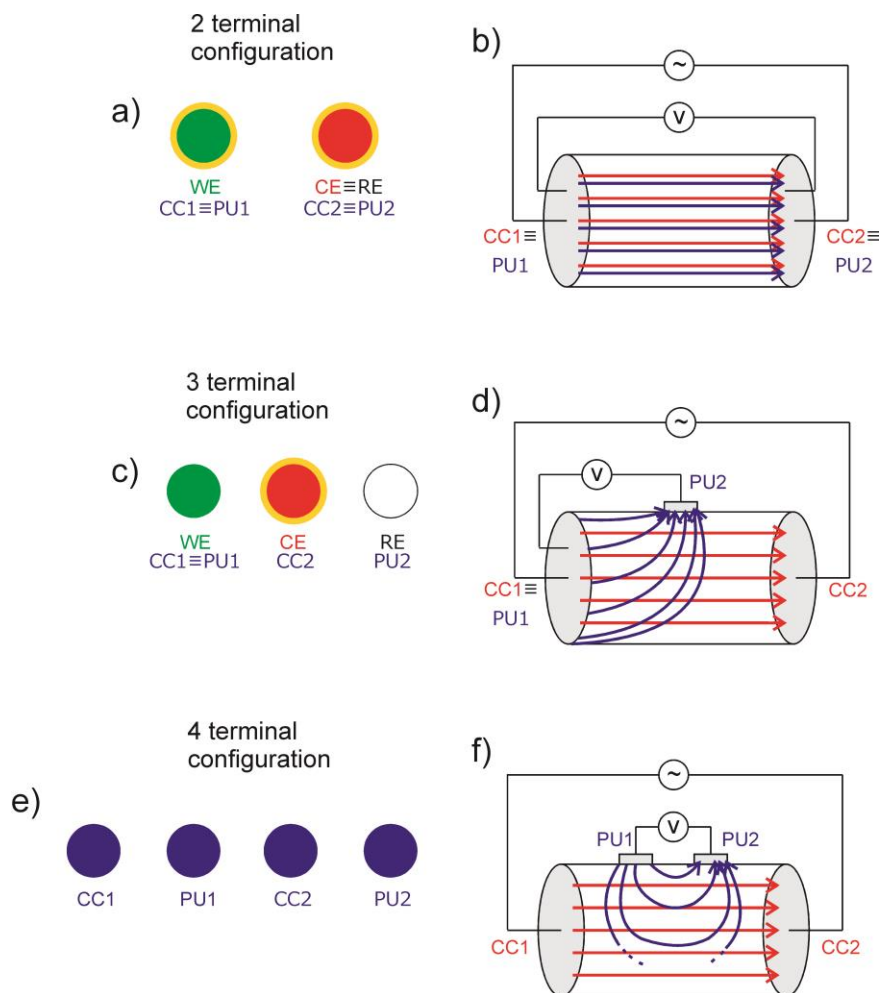


**Fig. S1.1.** Schematics of 2T (a), 3T (c) and 4T (e) configurations and their respective sensitivity fields (b, d, f) for a generic cylindrical conductor. In electrochemical analysis WE (green) is the working electrode, CE (red) is the counter electrode, RE (white) is the reference electrode. In bioimpedance measurements CC1 and CC2 form the current-carrying couple; PU1 and PU2 form the voltage pick-up couple. Polarisation impedance ( $Z_p$ ) at the electrode surface is reported in yellow, if present (a, c, e). For the representation of the sensitivity fields (b, d, f), red and blue arrows refer to the direction of CC and PU electric fields, respectively.

In 2T configuration (Fig. S1.1a, b), the same electrode pair serves both as CC and PU and the measured impedance typically includes the polarisation impedance ( $Z_p$ ) at both electrodes surface (Fig. S1a). Both CC electrodes are into the sensitivity zone for the measurement (Fig. S1b) and, therefore, the measured impedance is affected by their  $Z_p$ s (which can be very much greater than the sample impedance itself). The sensitivity field is always positive.

In 3T configuration (Fig. S1.1c, d), one electrode is common between the CC and PU couple (i.e. the counter electrode, CE). In other words, the CE is the only CC electrode which is still into the sensitivity zone for the measurement (Fig. S1.1d) and hence, the measured impedance is affected by its  $Z_p$  (which also reflects the sample volume in its close proximity, Fig. S1.1c).

In 4T configuration (Fig. S1.1e, f), two separate couples of CC and PU electrodes are used. This configuration eliminates all  $Z_p$  contributions; hence it is typically used for physiological measurements, where a specific focus on the mere properties of the biological sample is needed. In 4T measurements, the CC couple is placed outside the sensitivity zone for the measurement (Fig. S1.1f) and, hence, the measured impedance is not affected by  $Z_{pCC}$ . Moreover, with ideal voltage amplifiers (amp), PU electrodes are not current carrying (Fig. S1.2) so that  $Z_{pPU}$  does not contribute to the measured impedance as well (Fig. S1.1e). Modern amps have input impedance ( $Z_{amp}$ ) in the GigaOhm range, meaning that they allow measuring impedance values up to the MegaOhm level without the sensitivity field being influenced by  $Z_{pCC}$ . This further explains why, in 4T configuration, the sensing is not influenced by  $Z_{pCC}$  even when CC and PU electrodes are close to each other.

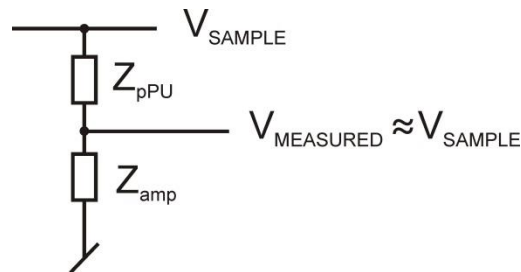


**Fig. S1.2.** Schematics of a 4T measurement. Using a 4T configuration, the sensing is focused only on the biological sample as the CC couple is placed outside the sensitivity zone for the measurement and the PU couple is not current-carrying. This means that the measured voltage ( $V_{MEASURED}$ ) is approximately the voltage across the sample ( $V_{SAMPLE}$ ).  $Z_{pPU}$  is the polarisation impedance of the PU electrodes and  $Z_{amp}$  the input impedance of the voltage amplifier.

In the beginning of impedance spectroscopy analysis it was mistakenly understood that the measured impedance reflects the impedivity (i.e., the property of “actual” impedance) of the sample bounded by the equipotential lines generated by current (or voltage) injection between the CC couple and passing through the PU couple. According to the *reciprocity theorem*, the measured impedance should be the same if the CC and PU couples are swapped. Therefore:

- the measurement sensitivity must be affected with some amount by all small sub-volumes in the sample (each of them displaying its own resistivity);
- small sub-volumes in the sample do not all equally contribute to the measured impedance;
- the measured impedance should be similar close to both electrode pairs;

- sub-volumes between CC and PU couples and close to the electrodes contribute more than sub-volumes far away from the electrodes.

The reciprocity theorem holds for all linear systems, i.e. those systems where the response to a sinusoidal perturbation is sinusoidal as well, with the same frequency of the input, but different amplitude and phase. Given the injected current between the CC couple as input ( $I$ ) and the measured voltage ( $E$ ) between the PU couple as output, the impedance ( $Z$ ) is the *transfer impedance* (or *transimpedance*) which can be approximated as the ratio between  $E$  and  $I$ :

$$Z \equiv \frac{E}{I} \quad [\Omega]$$

Since  $Z$  is a transfer function, it cannot be used for calculating sample properties as conductivity ( $\sigma$ ), resistivity ( $\rho$ ) and relative permittivity ( $\epsilon_r$ ), with the exception of homogeneous and uniform materials.

Resistivity ( $\rho$ ) is defined as the ratio between the voltage ( $E$ ) and the current density lines ( $J$ ), as described by the Ohm's law:

$$\rho = \frac{E}{J} \quad [\Omega \cdot \text{m}]$$

Hence,  $Z$  can be written as following:

$$Z = \iiint \rho \cdot \frac{J_{CC} \cdot J_{PU}}{I_{CC} \cdot I_{PU}} dv \quad [\Omega]$$

meaning that the total measured impedance is the sum of all local  $\rho$  values from each small sub-volume in the sample.

The sensitivity ( $S$ ) of an impedance measurement is the scalar value representing the CC current density lines ( $J_{CC}$ ) projection on the PU current density lines ( $J_{PU}$ ).  $S$  is affected with some amount by all sample sub-volumes and, as previously explained, it does not depend on  $\rho$  value:

$$S = \frac{J_{CC} \cdot J_{PU}}{I_{CC} \cdot I_{PU}} \quad [\text{m}^{-4}]$$

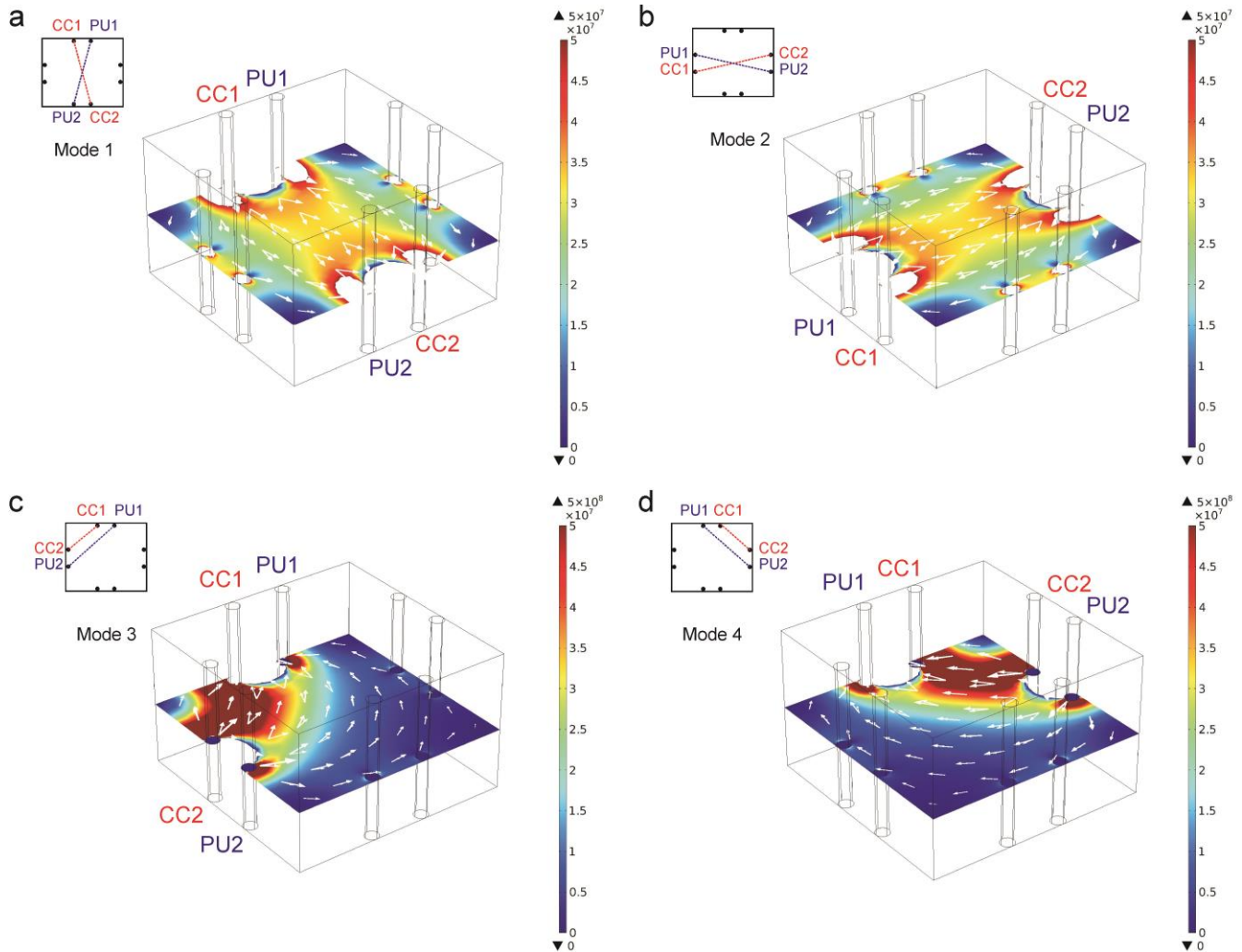
$S$  is a positive (or negative) value if measured impedance increases (or decreases) when the impedivity of that region increases. This may be clearly seen by drawing the current density vectors between the CC and PU couples. If they are:

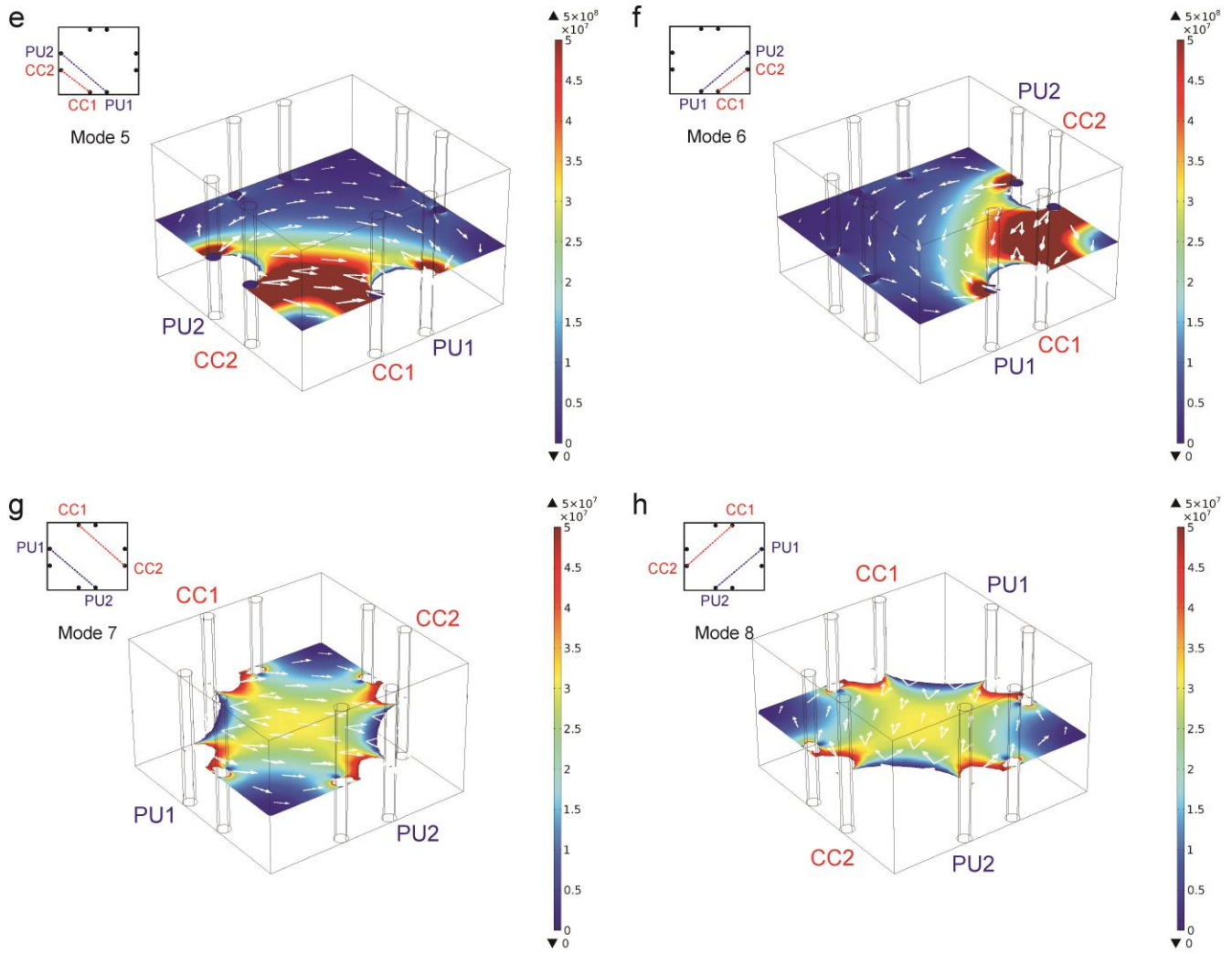
- in the same direction,  $S$  will be positive,
- superimposed,  $S$  will be maximum (since  $\cos 0 = 1$ , as for 2T measurements),
- in the opposite direction,  $S$  will be negative,
- in perpendicular direction,  $S$  will be 0 (since  $\cos 90 = 0$ ).

By means of finite element (FE) analysis, it is possible to estimate the  $S$  value weighted for the resistivity ( $\rho$ ) contribution of all sub-volumes in the sample, therefore estimating the local contribution of each sub-volume to the measured impedance. This latter is often called "volume impedance density" ( $VID$ ).  $VID$  is the integration of  $S$  over the entire sample volume and, accordingly, it corresponds to the expression defining the transimpedance,  $Z$ .

## Section S2. FE simulation of alternative measurement chamber size and electrode distance

Using the rectangular geometry showed in the manuscript, the sensitivity volume is “stretched” inside the measurement chamber, with symmetry between modes focusing on corners (3, 4, 5 and 6) and between modes 7 and 8. Using a square chamber with 16 mm side (Fig. S2.1), the simulated impedance values are one order of magnitude lower ( $10^7 \Omega$ ) than those obtained with the chosen rectangular geometry ( $10^8 \Omega$ ) because the current path is shorter. Moreover, the distribution of the sensitivity field (S) has the same global behavior as for the chosen rectangular geometry, with no advantage in using a square geometry.

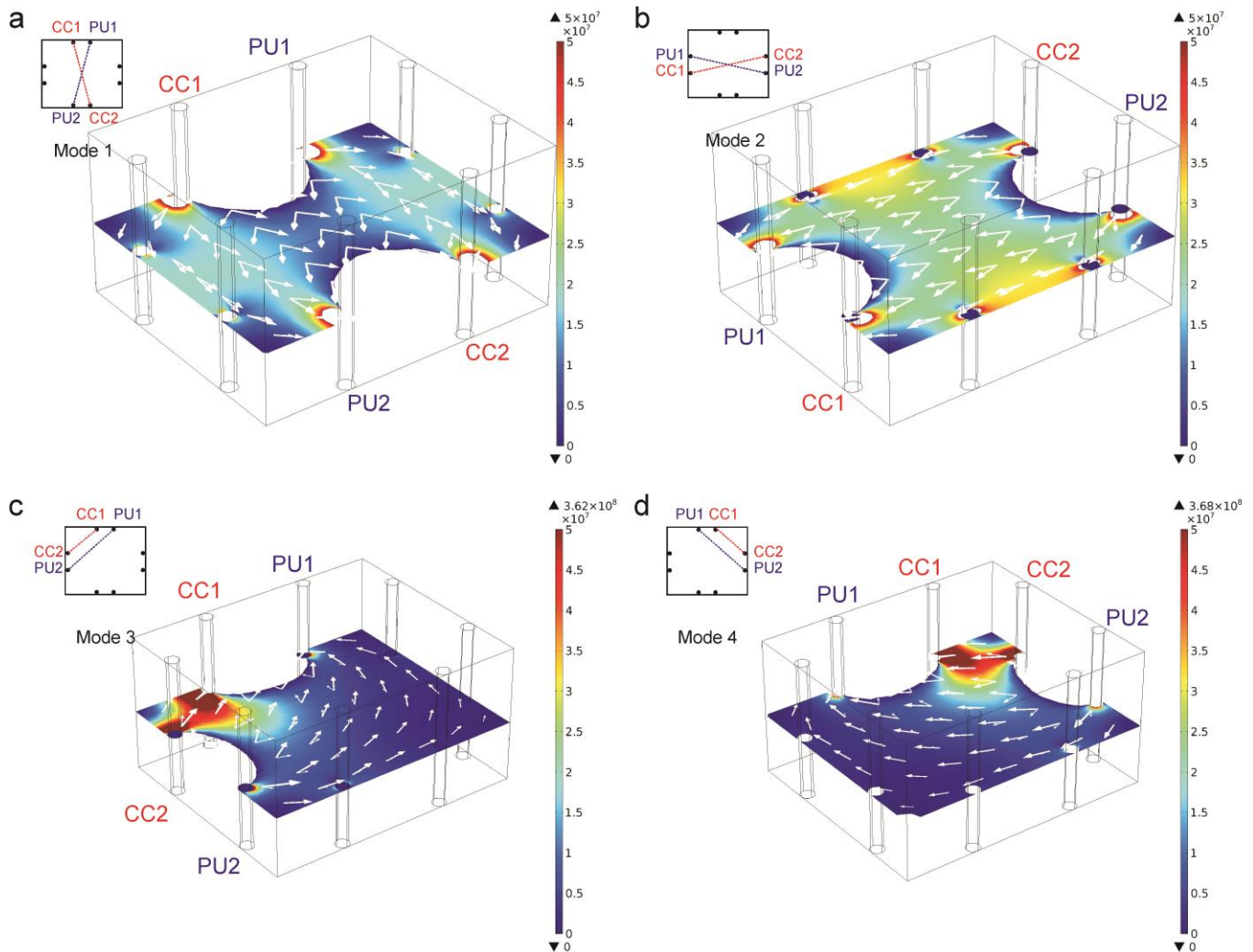


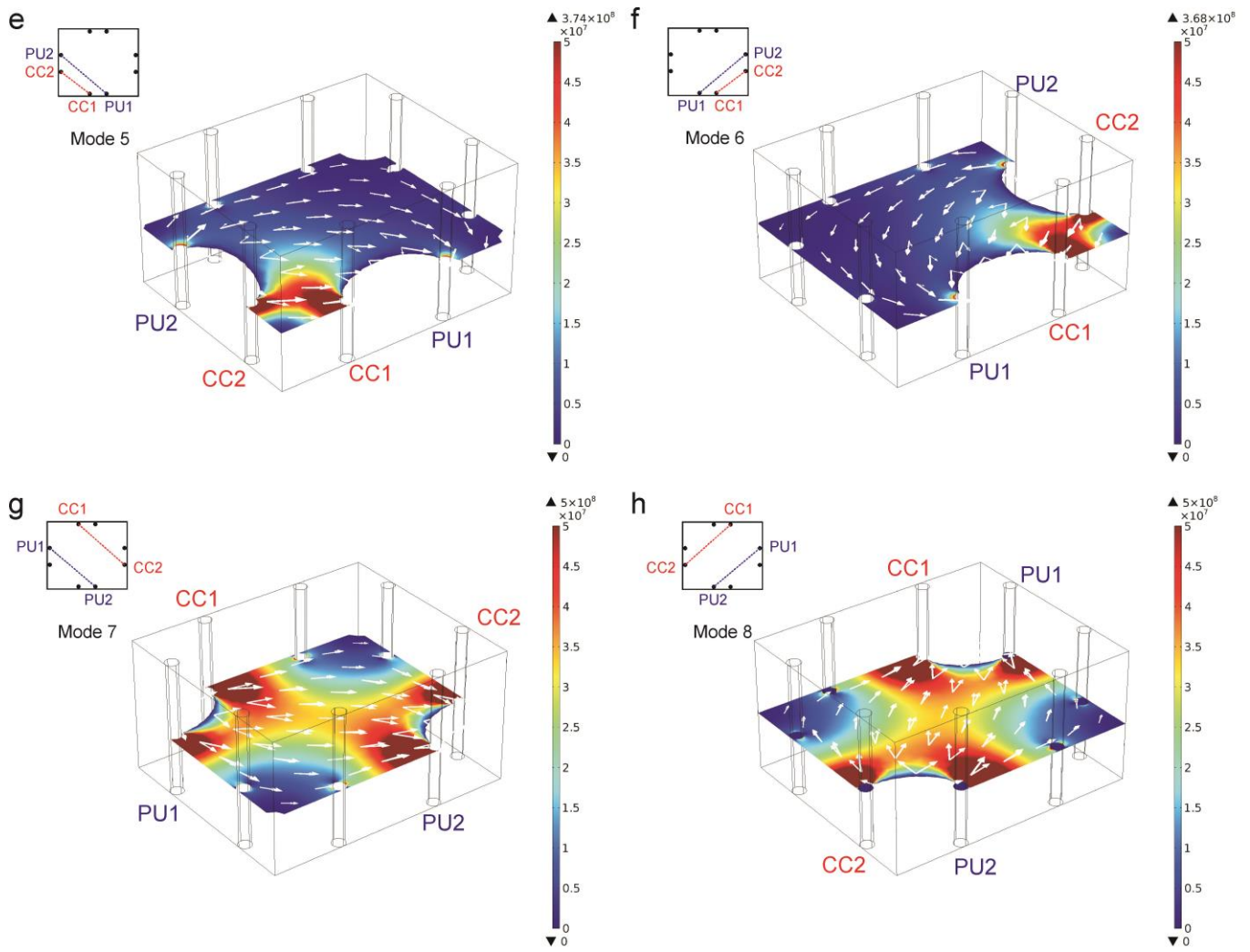


**Fig. S2.1.** FE analysis for  $S$  [m<sup>-4</sup>] distribution using a square measurement chamber of 16 mm side, where the electrodes are placed 4 mm apart from each other on each side of the chamber. (a) Mode 1, (b) mode 2, (c) mode 3, (d) mode 4, (e) mode 5, (f) mode 6, (g) mode 7 and (h) mode 8.

Using the eight different modes for electrodes placed at a centre-to-centre distance of 8 mm (Fig. S2.2) and 12 mm (data not shown) on each measurement chamber side, the following conclusions were drawn.

- Modes 1 and 2: When increasing the electrode distance, the contribution from volumes associated with negative sensitivity becomes larger.
- Modes 3, 4, 5 and 6: Doubling the electrode distance, the focus on corners becomes extremely narrow and the sensitivity volume is extremely reduced.
- Modes 7 and 8: When increasing the electrode distance, mode 7 and 8 give a good sensitivity profile. However it is crucial to find a good compromise in terms of positive sensitivity field among all the different modes in order to place the electrodes in a common position to all of them. Therefore, the solution presented in the manuscript (chamber size  $16 \times 19 \times 10 \text{ mm}^3$  with electrode couples where electrodes are placed 4 mm apart from each other on each side of the chamber) is definitely the best achievable one.

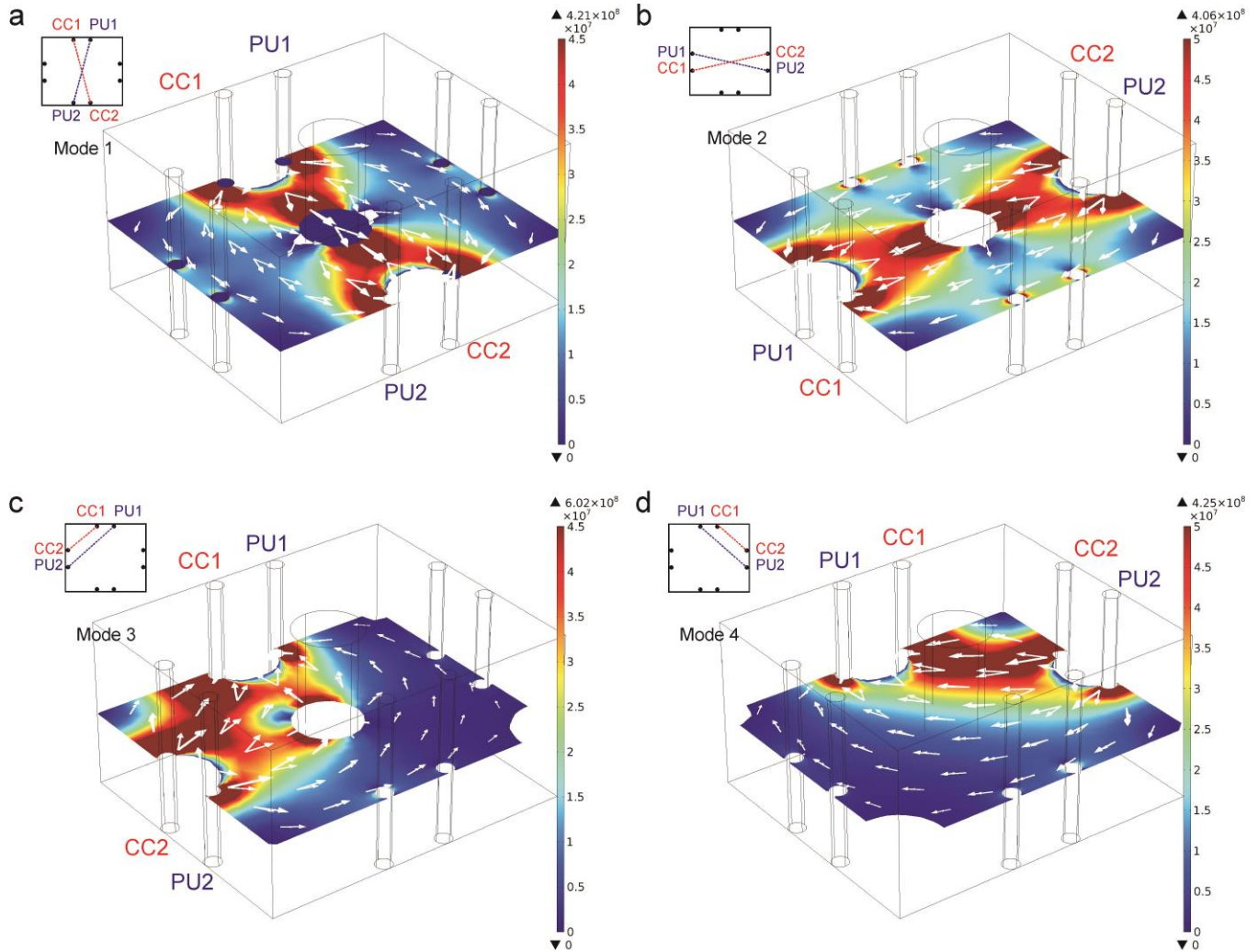


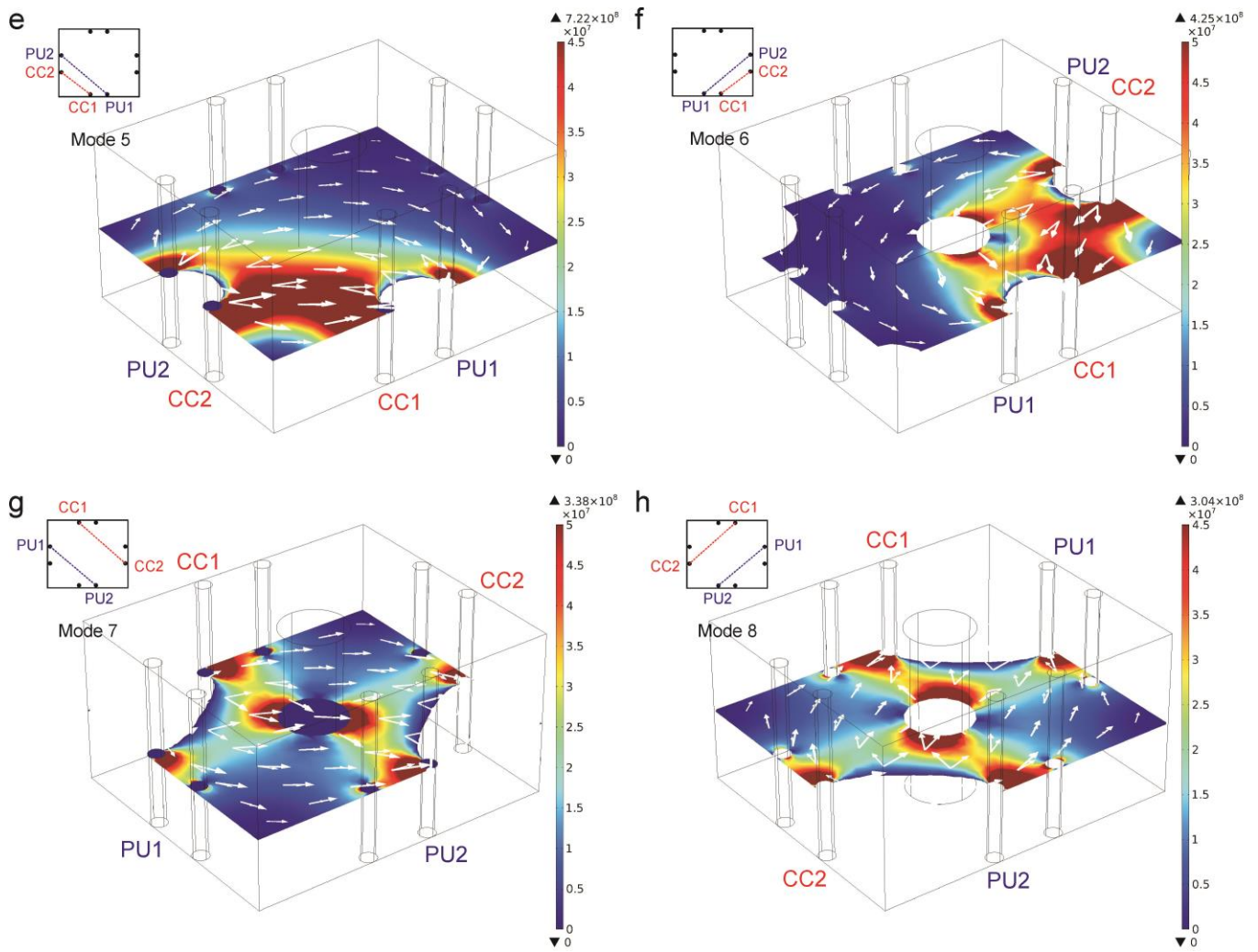


**Fig. S2.2.** FE analysis for  $S$  [ $\text{m}^{-4}$ ] distribution using a rectangular measurement chamber of  $16 \times 19 \times 10 \text{ mm}^3$ , where the electrodes are placed 8 mm apart from each other on each side of the chamber. (a) Mode 1, (b) mode 2, (c) mode 3, (d) mode 4, (e) mode 5, (f) mode 6, (g) mode 7 and (h) mode 8.

### Section S3. FE simulation of metal and plastic phantoms

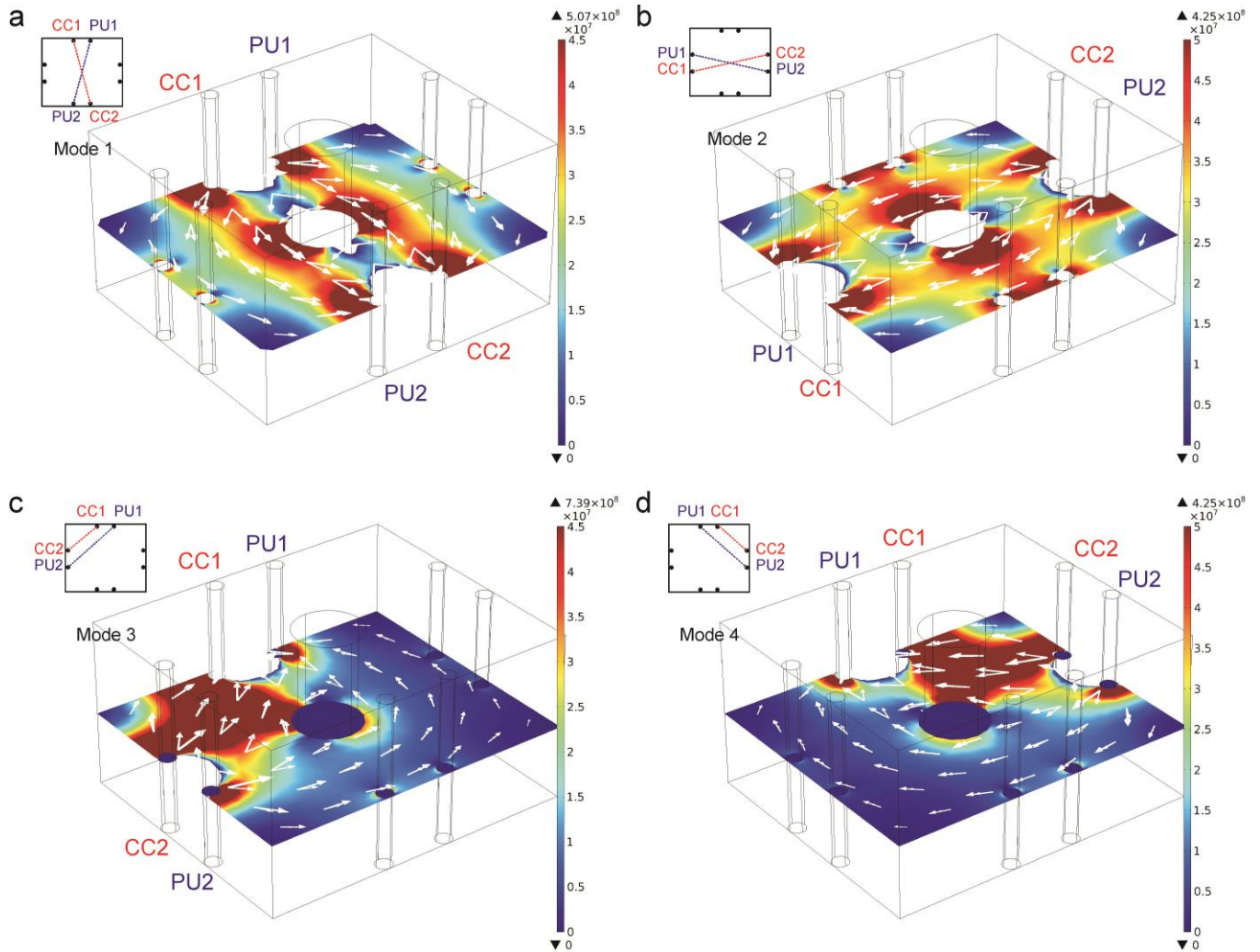
FE simulations were performed in presence of a vertical metal phantom (diameter of 4 mm and length of 10 mm,  $\sigma = 4.032 \times 10^6$  S/m and  $\epsilon_r = 1$ ) placed in the centre of the measurement chamber filled with saline solution ( $\sigma = 1.3$  S/m and  $\epsilon_r = 1$ ), Fig. S3.1. As expected from the theory described in Section S1, when the metal phantom is placed in volumes associated with positive  $S$ , the measured impedance decreases. Accordingly, as consequence of the Ohm's law for a volume conductor, a certain amount of current will be preferably absorbed by the phantom with a decrease in the measured impedance. FE simulations of a metal phantom placed in one corner of the measurement chamber (not reported) were consistent with the ones for the centre, here reported.





**Fig. S3.1.** FE simulations for  $S$  [ $\text{m}^{-4}$ ] distribution in presence of a vertical metal phantom placed in the centre of the measurement chamber filled with saline solution: (a) mode 1, (b) mode 2, (c) mode 3, (d) mode 4, (e) mode 5, (f) mode 6, (g) mode 7 and (h) mode 8.

FE simulations were performed in presence of a vertical plastic phantom (diameter of 4 mm and length of 10 mm,  $\sigma = 1 \times 10^{-19}$  S/m and  $\epsilon_r = 1$ ) placed in the centre of the measurement chamber filled with saline solution ( $\sigma = 1.3$  S/m and  $\epsilon_r = 1$ ), Fig. S3.2. As expected from the theory described in Section S1, when the plastic phantom is placed in volumes associated with positive  $S$ , the measured impedance increases. Accordingly, as consequence of the Ohm's law for a volume conductor, the current path will tend to "avoid" the insulating phantom and will preferably go through the more conductive saline solution around. FE simulations for a plastic phantom placed in one corner of the measurement chamber (not shown) were consistent with the ones for the centre, here reported.



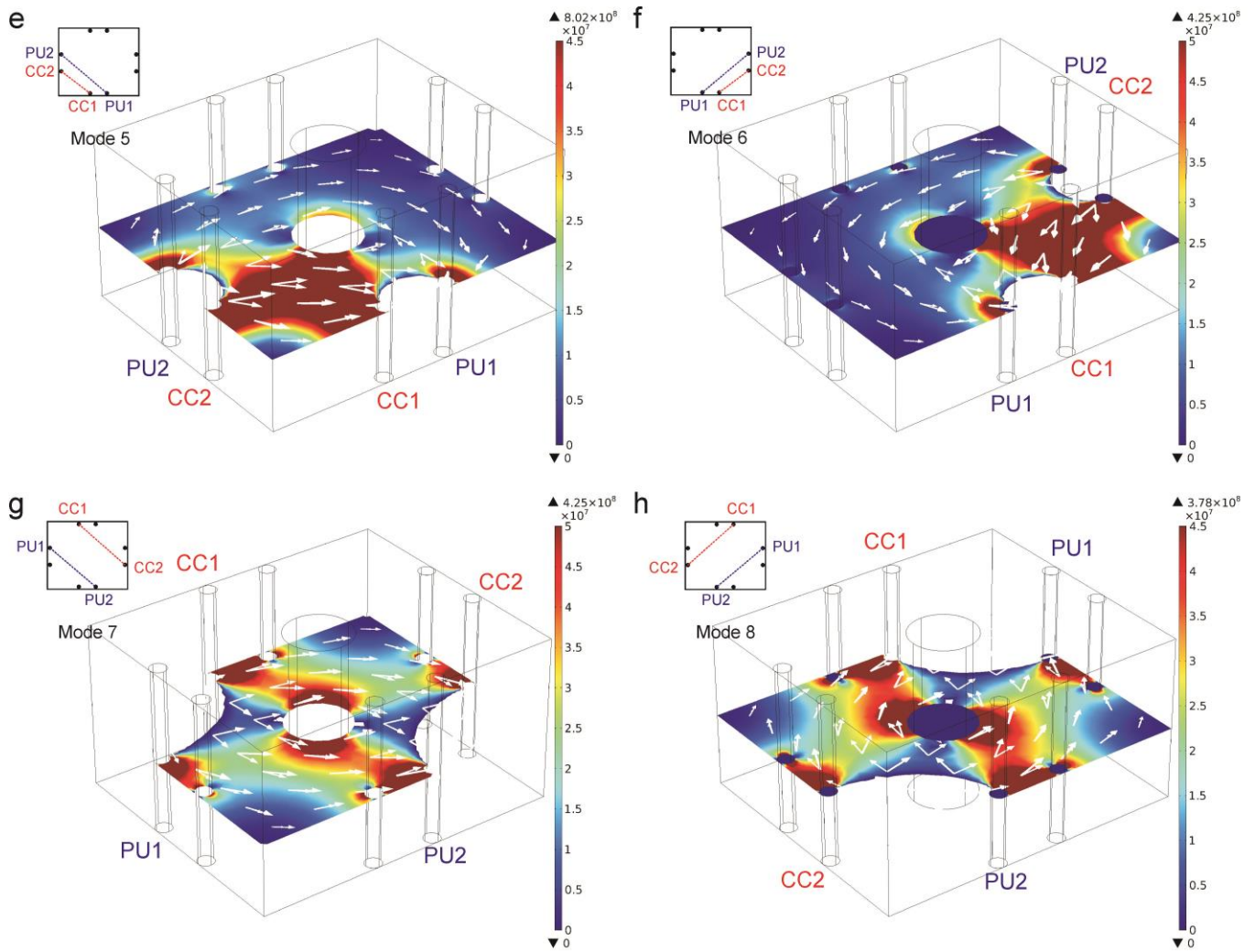


**Fig. S3.2.** FE simulations for  $S$  [ $\text{m}^4$ ] distribution in presence of a vertical plastic phantom placed in the centre of the measurement chamber filled with saline solution: (a) mode 1, (b) mode 2, (c) mode 3, (d) mode 4, (e) mode 5, (f) mode 6, (g) mode 7 and (h) mode 8.

## Section S4. Summary of phantom experiments

Phantom experiments are typically used to evaluate the sensitivity and accuracy of the response of an imaging device to an object which mimics the properties of biological tissues and organs. Fields of application are, e.g., electrical impedance tomography (EIT), magnetic resonance imaging (MRI), computed tomography (CT) and ultrasounds. A phantom may consist of real animal or vegetal tissues (e.g. carrot, potato, ...), or any other kind of material (e.g. hydrogel) able to reproduce the physical properties of the final biological sample to be measured. Since phantom experiments allow characterising the spatial sensitivity of an imaging device, this approach was successfully applied to determine the spatial sensitivity of our 3D bioimpedance-based method. The simulated sensitivity fields (S) for the eight 4T modes were validated with phantom experiments using metal and plastic cylinders. Table S4 shows the relative impedance variation for 4 mm metal and plastic phantoms placed in different positions (centre and corners) inside the measurement chamber filled with saline solution of standard conductivity 1.3 S/m. The relative impedance variation was calculated as difference between the measured impedance in presence of the cylinder and the measured impedance for the saline solution only. For all phantom experiments, characterisation data are presented as an average of three individual experiments in each chamber using fresh solution and rinsing the phantom with Milli-Q water (average  $\pm$  s.e.m., n = 12).

**Table S4.** Impedance variation at 250 kHz for a 4 mm metal and plastic phantoms placed in different positions inside the measurement chamber filled with saline solution of conductivity 1.3 S/m (average  $\pm$  s.e.m., n = 12).

<b>MODE 1</b>		
<b>Position</b>	<b>Metal (Ohm)</b>	<b>Plastic (Ohm)</b>
<i>Centre</i>	-6.4 $\pm$ 0.5	6.3 $\pm$ 0.4
<i>Top Left</i>	-5.7 $\pm$ 0.5	5.1 $\pm$ 1.3
<i>Top Right</i>	-6.8 $\pm$ 0.4	2.8 $\pm$ 0.6
<i>Bottom Left</i>	-6.4 $\pm$ 0.5	1.5 $\pm$ 0.6
<i>Bottom Right</i>	-6.7 $\pm$ 0.4	1.4 $\pm$ 0.6

<b>MODE 2</b>		
<b>Position</b>	<b>Metal (Ohm)</b>	<b>Plastic (Ohm)</b>
<i>Centre</i>	-7.4 $\pm$ 2.0	5.7 $\pm$ 2.0
<i>Top Left</i>	-6.5 $\pm$ 0.7	8.9 $\pm$ 0.8
<i>Top Right</i>	-7.4 $\pm$ 0.8	5.1 $\pm$ 1.6
<i>Bottom Left</i>	-7.0 $\pm$ 0.8	3.5 $\pm$ 1.4
<i>Bottom Right</i>	-8.5 $\pm$ 0.6	7.8 $\pm$ 2.0

**MODE 3**

<b>Position</b>	<b>Metal (Ohm)</b>	<b>Plastic (Ohm)</b>
<i>Centre</i>	$-3.9 \pm 0.4$	$1.0 \pm 0.4$
<i>Top Left</i>	$-12.5 \pm 0.5$	$15.9 \pm 0.7$
<i>Top Right</i>	$-2.9 \pm 0.4$	$0.5 \pm 0.4$
<i>Bottom Left</i>	$-3.6 \pm 0.5$	$0.3 \pm 0.5$
<i>Bottom Right</i>	$-2.2 \pm 0.4$	$-4.7 \pm 1.4$

**MODE 4**

<b>Position</b>	<b>Metal (Ohm)</b>	<b>Plastic (Ohm)</b>
<i>Centre</i>	$-4.4 \pm 0.5$	$2.8 \pm 0.5$
<i>Top Left</i>	$1.8 \pm 0.7$	$4.3 \pm 0.4$
<i>Top Right</i>	$-11.9 \pm 0.5$	$16.0 \pm 0.6$
<i>Bottom Left</i>	$0.0 \pm 0.6$	$-0.8 \pm 0.4$
<i>Bottom Right</i>	$-3.4 \pm 0.6$	$1.4 \pm 0.4$

**MODE 5**

<b>Position</b>	<b>Metal (Ohm)</b>	<b>Plastic (Ohm)</b>
<i>Centre</i>	$-3.9 \pm 0.9$	$1.6 \pm 0.8$
<i>Top Left</i>	$-4.1 \pm 0.6$	$2.2 \pm 0.4$
<i>Top Right</i>	$-2.8 \pm 0.5$	$-3.3 \pm 0.6$
<i>Bottom Left</i>	$-13.9 \pm 0.4$	$11.3 \pm 0.7$
<i>Bottom Right</i>	$-3.6 \pm 0.3$	$3.7 \pm 0.5$

**MODE 6**

<b>Position</b>	<b>Metal (Ohm)</b>	<b>Plastic (Ohm)</b>
<i>Centre</i>	$-4.1 \pm 0.4$	$2.3 \pm 1.3$
<i>Top Left</i>	$-1.6 \pm 0.6$	$0.6 \pm 0.4$
<i>Top Right</i>	$-4.0 \pm 0.7$	$2.9 \pm 0.5$
<i>Bottom Left</i>	$-4.1 \pm 0.4$	$0.8 \pm 0.4$
<i>Bottom Right</i>	$-13.4 \pm 0.3$	$12.5 \pm 0.7$

**MODE 7**

<b>Position</b>	<b>Metal (Ohm)</b>	<b>Plastic (Ohm)</b>
<i>Centre</i>	$-7.2 \pm 0.8$	$5.7 \pm 1.4$
<i>Top Left</i>	$-3.6 \pm 1.0$	$-6.5 \pm 0.7$
<i>Top Right</i>	$-5.6 \pm 0.6$	$2.0 \pm 0.5$
<i>Bottom Left</i>	$-5.8 \pm 0.4$	$0.3 \pm 2.2$
<i>Bottom Right</i>	$-2.0 \pm 0.4$	$-6.8 \pm 0.6$

**MODE 8**

<b>Position</b>	<b>Metal (Ohm)</b>	<b>Plastic (Ohm)</b>
<i>Centre</i>	$-7.7 \pm 0.6$	$4.6 \pm 0.9$
<i>Top Left</i>	$-7.4 \pm 0.6$	$3.3 \pm 0.5$
<i>Top Right</i>	$-3.0 \pm 0.4$	$-3.4 \pm 0.4$
<i>Bottom Left</i>	$-4.4 \pm 0.5$	$-5.7 \pm 0.7$
<i>Bottom Right</i>	$-7.0 \pm 0.4$	$1.6 \pm 0.4$

## Section S5. Bioimpedance sensing of 5% (w/v) bulk gelatin scaffolds

Table S5 shows impedance ( $|Z|$ , real  $Z$  and imaginary  $Z$ ) and phase angle ( $\varphi$ ) values at 250 kHz for 5% (w/v) bulk gelatin scaffolds of  $16 \times 19 \times 6.6 \text{ mm}^3$  size.

$|Z|$  was always equal to real  $Z$ , showing a decrease over time. This behaviour is opposite to what was expected, but can be explained when considering the cell culture medium diffusion through the scaffold over time. In fact, since polymerisation is associated with lower ionic mobility within the gelatin matrix, this would have been expected to decrease the scaffold conductivity, with an increase in the measured impedance. However, cell culture medium was added on top of the scaffolds at  $t_0$  and a diffusion rate of  $0.41 \mu\text{m}/\text{sec}$  was measured through the scaffold. This means that after 2 hours, the cell culture medium went through almost a half of the scaffold height and, after 4 hours, it went almost completely through it. Cell culture medium has high conductivity (1.6 - 1.8 S/m; C. Canali et al. 2015, H. Hsu et al. 2010, McIntosh et al. 2003), hence lowering the measured impedance over time.

Imaginary  $Z$  was almost constant over time and this may entail that the gelatin scaffolds made with our protocol have mainly a resistive behavior. Accordingly, the phase angle was almost zero and constant over time.

**Table S5.** Impedance ( $|Z|$ , real  $Z$  and imaginary  $Z$ ) and phase angle values at 250 kHz for 5% (w/v) bulk gelatin scaffolds of  $16 \times 19 \times 6.6 \text{ mm}^3$  size. Data are presented as average  $\pm$  s.e.m.,  $n = 21$ .

<b>MODE 1</b>			
	<b><math>t_0</math> (0 hours)</b>	<b><math>t_1</math> (2 hours)</b>	<b><math>t_2</math> (4 hours)</b>
$ Z $ (Ohm)	$48.2 \pm 3$	$45.4 \pm 5.5$	$40.8 \pm 7.2$
$Z_{Re}$ (Ohm)	$48.2 \pm 3$	$45.4 \pm 5.5$	$40.8 \pm 7.2$
$Z_{Im}$ (Ohm)	$0.7 \pm 0.2$	$0.7 \pm 0.2$	$1.0 \pm 0.1$
$\varphi$ (Deg.)	$0.0 \pm 0.0$	$0.0 \pm 0.0$	$0.0 \pm 0.0$

<b>MODE 2</b>			
	<b><math>t_0</math> (0 hours)</b>	<b><math>t_1</math> (2 hours)</b>	<b><math>t_2</math> (4 hours)</b>
$ Z $ (Ohm)	$69.8 \pm 5.3$	$64.8 \pm 6.0$	$61.2 \pm 8.2$
$Z_{Re}$ (Ohm)	$69.8 \pm 5.3$	$64.8 \pm 6.0$	$61.2 \pm 8.2$
$Z_{Im}$ (Ohm)	$1.2 \pm 0.16$	$1.2 \pm 0.1$	$1.2 \pm 0.1$
$\varphi$ (Deg.)	$0.0 \pm 0.0$	$0.0 \pm 0.0$	$0.0 \pm 0.0$

<b>MODE 3</b>			
	<b><math>t_0</math> (0 hours)</b>	<b><math>t_1</math> (2 hours)</b>	<b><math>t_2</math> (4 hours)</b>
$ Z $ (Ohm)	$43.2 \pm 2.8$	$42.6 \pm 4.4$	$37.0 \pm 5.7$
$Z_{Re}$ (Ohm)	$43.2 \pm 2.8$	$42.6 \pm 4.4$	$37.0 \pm 5.7$
$Z_{Im}$ (Ohm)	$0.9 \pm 0.1$	$0.9 \pm 0.1$	$0.8 \pm 0.1$
$\varphi$ (Deg.)	$0.0 \pm 0.0$	$0.0 \pm 0.0$	$0.0 \pm 0.0$

**MODE 4**

	<b>t<sub>0</sub> (0 hours)</b>	<b>t<sub>1</sub> (2 hours)</b>	<b>t<sub>2</sub> (4 hours)</b>
$ Z $ (Ohm)	$57.8 \pm 5.4$	$38.0 \pm 3.8$	$40.7 \pm 5.4$
$Z_{Re}$ (Ohm)	$57.8 \pm 5.4$	$38.0 \pm 3.8$	$40.7 \pm 5.4$
$Z_{Im}$ (Ohm)	$1.0 \pm 0.1$	$0.8 \pm 0.1$	$0.7 \pm 0.1$
$\varphi$ (Deg.)	$0.0 \pm 0.0$	$0.0 \pm 0.0$	$0.0 \pm 0.0$

**MODE 5**

	<b>t<sub>0</sub> (0 hours)</b>	<b>t<sub>1</sub> (2 hours)</b>	<b>t<sub>2</sub> (4 hours)</b>
$ Z $ (Ohm)	$44 \pm 3.2$	$47.4 \pm 5.8$	$36.7 \pm 6.2$
$Z_{Re}$ (Ohm)	$44 \pm 3.2$	$47.4 \pm 5.8$	$36.7 \pm 6.2$
$Z_{Im}$ (Ohm)	$0.9 \pm 0.2$	$0.8 \pm 0.1$	$0.7 \pm 0.1$
$\varphi$ (Deg.)	$0.0 \pm 0.0$	$0.0 \pm 0.0$	$0.0 \pm 0.0$

**MODE 6**

	<b>t<sub>0</sub> (0 hours)</b>	<b>t<sub>1</sub> (2 hours)</b>	<b>t<sub>2</sub> (4 hours)</b>
$ Z $ (Ohm)	$55.8 \pm 6.5$	$38.1 \pm 4.1$	$38.7 \pm 6.0$
$Z_{Re}$ (Ohm)	$55.8 \pm 6.5$	$38.1 \pm 4.1$	$38.71 \pm 6.0$
$Z_{Im}$ (Ohm)	$0.9 \pm 0.1$	$0.7 \pm 0.1$	$0.7 \pm 0.1$
$\varphi$ (Deg.)	$0.0 \pm 0.0$	$0.0 \pm 0.0$	$0.0 \pm 0.0$

**MODE 7**

	<b>t<sub>0</sub> (0 hours)</b>	<b>t<sub>1</sub> (2 hours)</b>	<b>t<sub>2</sub> (4 hours)</b>
$ Z $ (Ohm)	$37.2 \pm 3.5$	$35.3 \pm 4.2$	$32.4 \pm 4.5$
$Z_{Re}$ (Ohm)	$37.2 \pm 3.5$	$35.3 \pm 4.2$	$32.4 \pm 4.5$
$Z_{Im}$ (Ohm)	$0.8 \pm 0.2$	$0.6 \pm 0.1$	$0.7 \pm 0.1$
$\varphi$ (Deg.)	$0.0 \pm 0.0$	$0.0 \pm 0.0$	$0.0 \pm 0.0$

**MODE 8**

	<b>t<sub>0</sub> (0 hours)</b>	<b>t<sub>1</sub> (2 hours)</b>	<b>t<sub>2</sub> (4 hours)</b>
$ Z $ (Ohm)	$40.1 \pm 3.6$	$33.2 \pm 3.8$	$31.3 \pm 4.5$
$Z_{Re}$ (Ohm)	$40.1 \pm 3.6$	$33.2 \pm 3.8$	$31.3 \pm 4.5$
$Z_{Im}$ (Ohm)	$0.9 \pm 0.2$	$0.6 \pm 0.1$	$0.7 \pm 0.1$
$\varphi$ (Deg.)	$0.0 \pm 0.0$	$0.0 \pm 0.0$	$0.0 \pm 0.0$

## Section S6. Biopedance sensing of 5% (w/v) gelatin cylinders and artificial 3D cell constructs

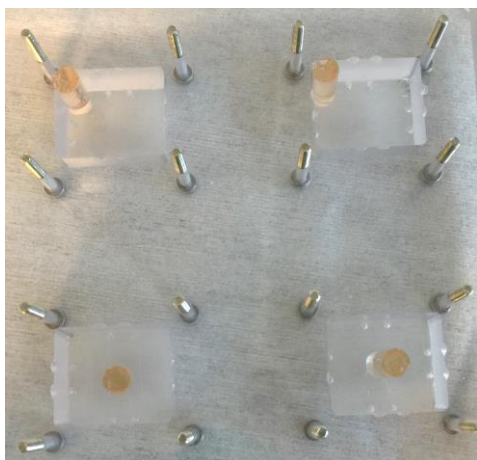


**Fig. S6.1.** Gelatin cylinders (with and without cells) were placed in two different positions inside the measurement chamber (centre or top left corner). Then, 2 mL of 5% (w/v) gelatin was casted around and let to polymerise for 2 hours at 37 °C in a humidified 5% CO<sub>2</sub> incubator. After gelatin polymerisation, the measurement chamber was filled with cell culture medium.

## S6A) Gelatin cylinders without cells

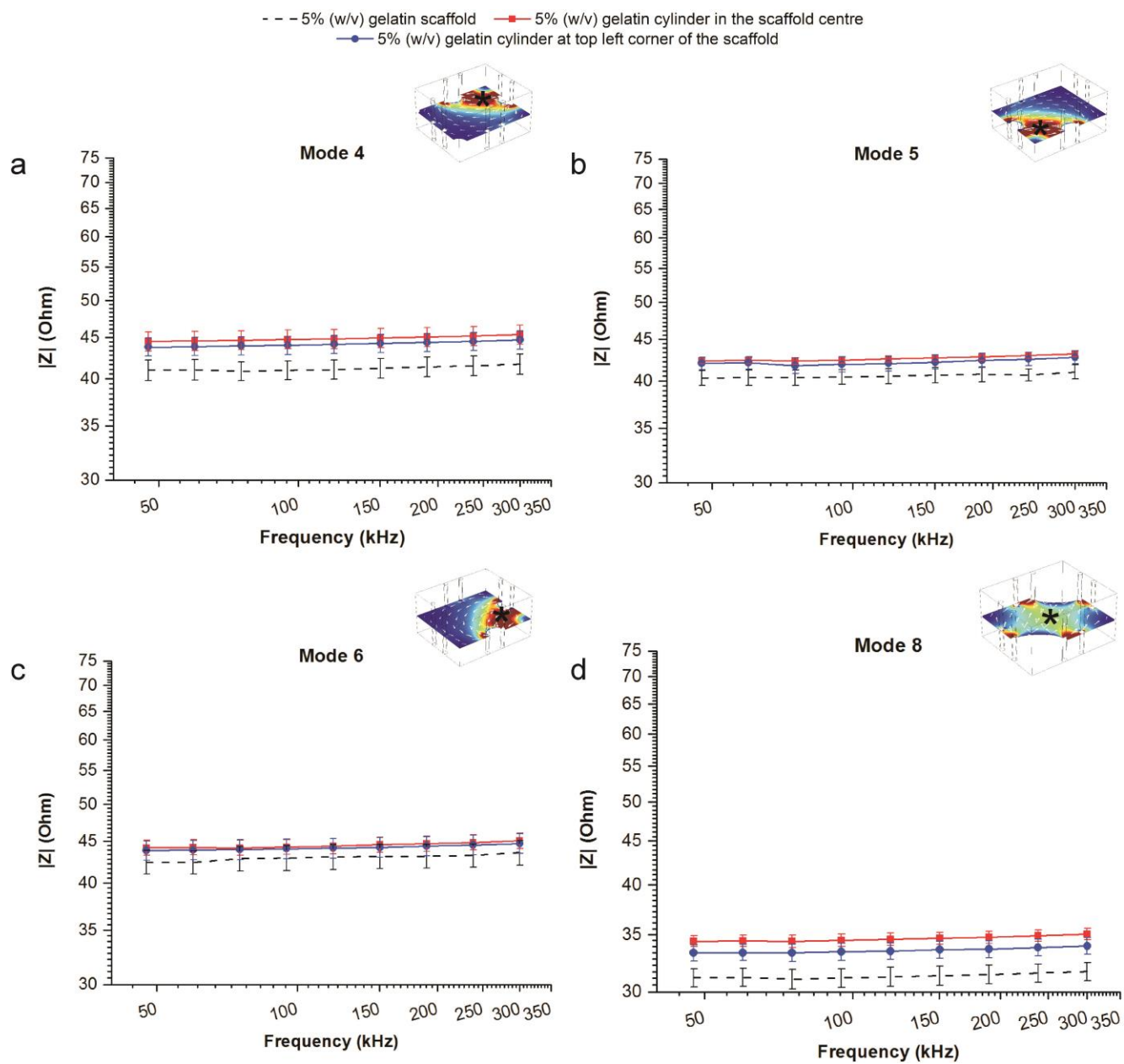


**Fig. S6.2.** Sensing of a 5% (w/v) gelatin cylinder embedded in bulk gelatin scaffold and placed either at the top left corner or in the centre: mode 4 (a), mode 5 (b), mode 6 (c), mode 8 (d). Data are compared with 5% (w/v) bulk gelatin scaffold (average  $\pm$  s.e.m.,  $n = 21$ ) and reported as average  $\pm$  s.e.m.,  $n = 6$ . The position of the main focus of each mode is indicated by an asterisk.

## S6B) Artificial 3D cell constructs

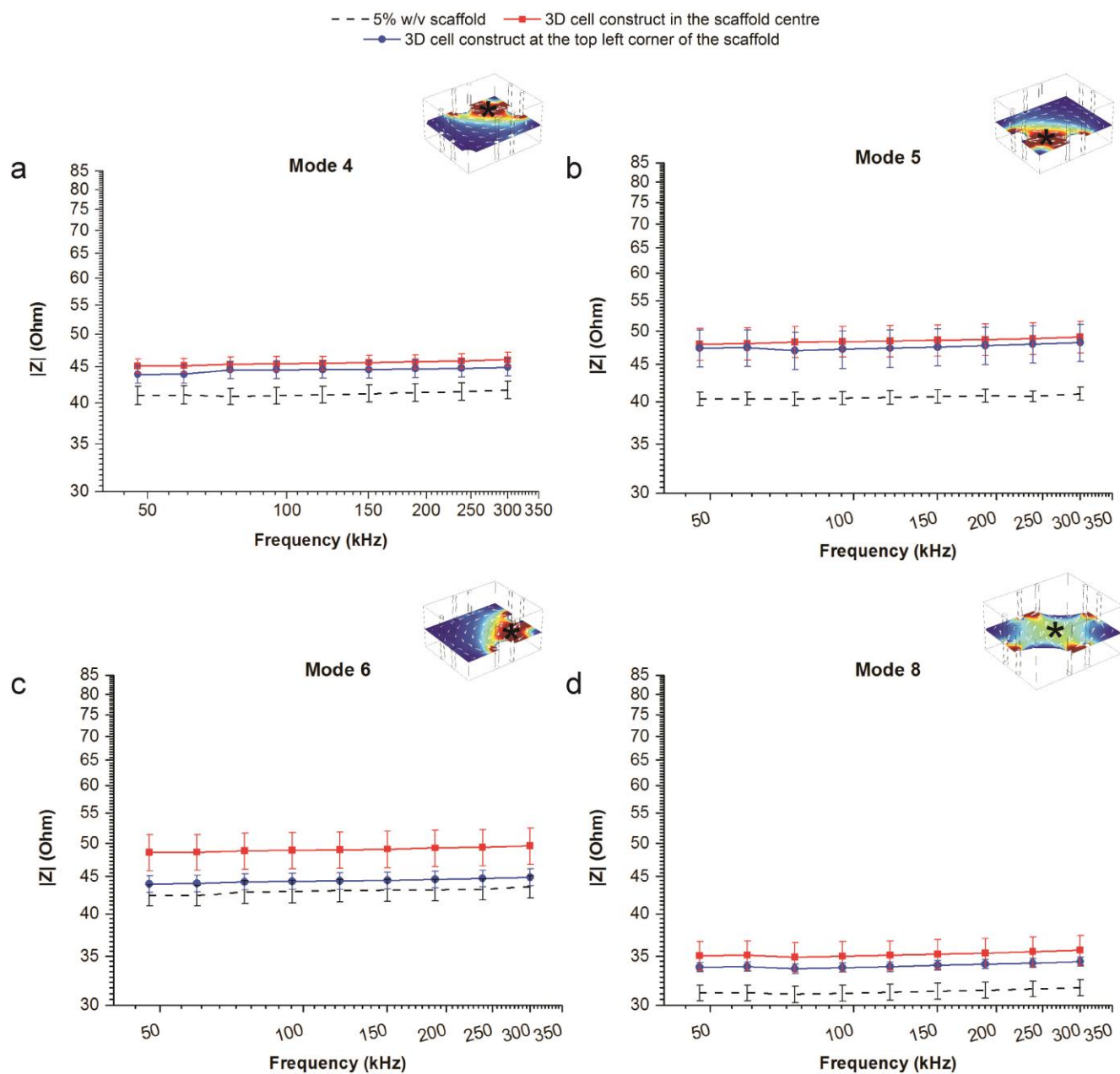


**Fig. S6.3.** Sensing of a 5% (w/v) gelatin cylinder containing  $10^7$  HepG2 cells as artificial 3D cell construct embedded in bulk gelatin scaffold and placed either at the top left corner or in the centre. Mode 4 (a), mode 5 (b), mode 6 (c), mode 8 (d). Data are compared with 5% (w/v) bulk gelatin scaffold (average  $\pm$  s.e.m.,  $n = 21$ ) and reported as average  $\pm$  s.e.m.,  $n = 6$ . The position of the main focus of each mode is indicated by an asterisk.